

Optimization of Gate Recess Step and Elimination of the Dome Effect for Highly Reliable and Reproducible Novel pHEMT Device

M. Mohamad Isa, N. Ahmad

School of Microelectronic Engineering, Universiti Malaysia
Perlis, Pauh Putra Campus, 02600 Arau, Perlis,
MALAYSIA.

*E-mail: muammar@unimap.edu.my

F. Packeer, M. Missous

Microelectronics And Nanostructures (M&N) Group,
School of E&EE, The University of Manchester,
M60 1QD, UNITED KINGDOM.

Abstract – We report a comprehensive etching study on gate recess processing step in Novel pseudomorphic High Electron Mobility Transistor (pHEMT) fabrication step. The conducted experiments focused on the etchant composition and elimination of the Cap layer residue (Dome Effect) at the etching trenches. The optimized processing flow using highly selective Succinic Acid is aimed for moderate Cap layer, with etching rate of 240 Å/min and InGaAs-InAlAs selectivity of 140 respectively. The percentage of the Dome height to etching depth is consistent to 30% throughout the etching surface, which can be further improved by controlling the etching time to the etch stop layer. The optimized processing steps will enhanced the device's robustness especially in the complete processing steps for Monolithic Microwave Integrated Circuit (MMIC) fabrication, tailored for high-gain and low noise applications in satellite communication.

Keywords—pHEMT, Schottky Contact, Ohmic Contact, MMIC, 2-DEG, pseudomorphic

I. INTRODUCTION

Over the past decade, Silicon based (Si-based) devices has serve their purposes as the main components in universal electronic gadgets and appliances. However, the tendency for better RF and microwave performances in today's applications has shifted the designer and manufacturers attention to more advanced materials, such as III-V compound [1,2]. InP pseudomorphic High Electron Mobility Transistor (pHEMT) for example, has proven itself to be the best three-terminal device for this purposes, especially for low noise applications at 2 – 1000 GHz [3]. Certainly, the III-V materials are the future candidates in the post sub-22 nm node [4]. The excellence in high-speed and low-noise characteristics are the resulting of the progression in consecutive layers of wide and narrow band-gap single crystals material growth using advanced technology such as Molecular Beam Epitaxy (MBE) [5-7].

Similar to other three-terminal Field Effect Transistor (FET) family, the pHEMT's gate is used to control the current flow between Source (S) and Drain (D) [8]. However, the control mechanism is done by manipulating the Schottky contact between the gate metal and the large band gap Schottky barrier layer. Such contact is made by etching the gate structure (gate recess process) at the narrow band-gap Cap layer, which conceal and protect the semiconductor surface. The narrow band-gap layer is also act as the metal penetration layer in forming the

Ohmic S-D contacts. The conventional pHEMT epitaxial layer is shown in in Fig. 1.

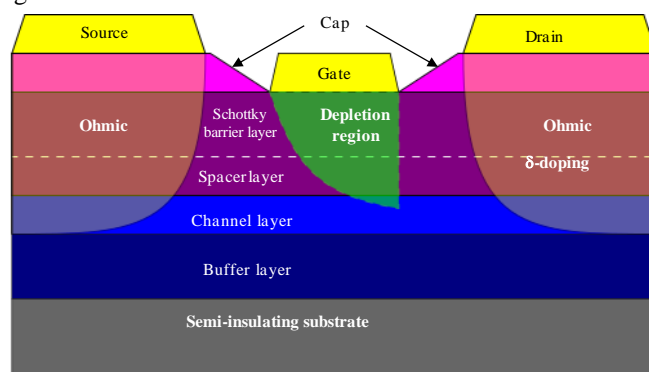


Fig. 1: Conventional pHEMT epitaxial layer

Here, the narrow band gap material is made from lattice matched InGaAs, whereas the wide band-gap materials is from lattice matched InAlAs compound.

The above figure shows the importance of a clean and good gate etching profile at the gate trenches. Incomplete Cap layer etching will leave Cap layer residue at the gate opening, and subsequently forms an unwanted Ohmic contact at the gate after the metal is deposited. The consequences of this contact-switch can be seen by the gate leakage current, whereby the carrier in the channel can easily slip to the outside circuit thru the unwanted metal-residue contact. In addition, previous study has shown that the gate recess depth and width has substantial effect on the device's threshold voltage (V_{th}), pinch voltage (V_p) and drain-source current (I_{DS}) [9].

Seeing the importance of this step, it is therefore reported in this paper the comprehensive study on the gate recess process. Even though almost similar experiment has been reported elsewhere [10-12], the information is limited only to the selection of etching agents and etching profiles. Therefore, in this paper we present an extensive study of the etchant preparation, and effect of each compound in the mixture to the etching profile. An additional yet significant finding in our work is the formation of "hump" at the etching structure, which directly correlate to the quality of the device's Schottky gate contact.

In order to achieve that, it is also important to choose the suitable etching agent that is highly selective and highly reproducible results. Even though the successfully fabricated devices have shown excellent DC and Radio Frequency (RF) performances, the commonly used Adipic Acid etchant has both process repeatability and reliability issues [13]. In contrast, Succinic Acid (SA) is a more advantageous solution due to its high selectivity and highly reproducible result [10]. Thus, parallel experiments is also being performed to investigate the etch rate and selectivity study of SA, so that the etching process is not a strong function of time and process variations.

II. SAMPLES PREPARATION

The initial experiments were conducted using two types of lattice match samples; the bulk Cap layer (InGaAs) and bulk Schottky layer (InAlAs). The samples are labelled as VMBE #1593 and VMBE #1594 respectively. The epitaxial structures for both samples were grown using MBE on a RIBER V100 System at The University of Manchester. The profiles for both epitaxial layers are depicted in Fig. 2 and Fig. 3. As illustrated in epitaxial layer profiles, the bulk InAlAs layer is protected by 50 Å of Cap layer to prevent the Aluminum oxidation in the material compound.

The samples were cleaned separately in an ultrasonic bath for 5 minutes successively with conventional cleaning agents; Trichloroethylene, Acetone and Isopropanol (IPA). An extra etching step on bulk InAlAs was used, where the samples is immersed for one minute in a non-selective orthophosphoric etch solution ($H_3PO_4:H_2O_2:H_2O$) with 3:1:50 composition for stripping off the cap layer. The steps is followed by rinsing the sample with running deionized (DI) water for another one minute good cleaning. All experiments were conducted at room temperature environment allowing the chemical compound to be used instantaneously. The etch structures were processes using conventional optical lithography and development. The resist used in this experiment is AZ® nLOF™ 2070 followed by development in MIF 326. The etching structures were chosen to be the MESA layer where with dimensions of approximately 100 µm.

8500 Å	$In_{0.53}Ga_{0.47}As$ undoped
500 Å	$In_{0.52}Al_{0.48}As$ undoped
	InP Substrate

Fig. 2: VMBE #1593 Epitaxial Layer

50 Å	$In_{0.53}Ga_{0.47}As$ undoped
8500 Å	$In_{0.52}Al_{0.48}As$ doped ($\sim 5 \times 10^{16} \text{ cm}^{-3}$)
	InP Substrate

Fig. 3 VMBE #1594 Epitaxial Layer

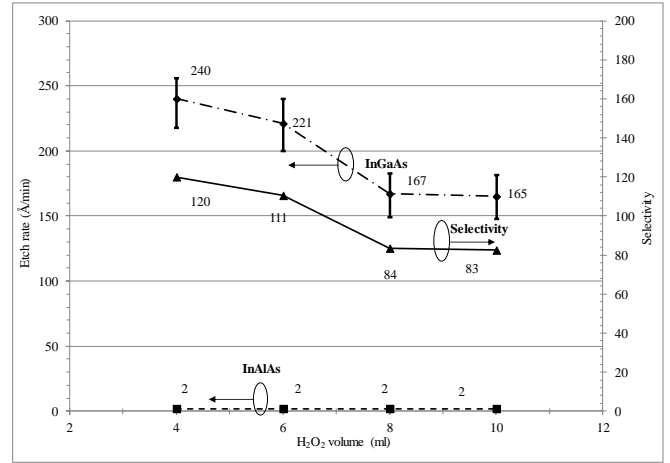


Fig. 4 Etch rate of lattice matched InGaAs and InAlAs and selectivity in different H_2O_2 composition. (DI volume = 50 ml and pH = 6)

III. RESULTS AND DISCUSSIONS

The experiment begin with the effect of peroxide (H_2O_2) composition on the semiconductor etch rate. In the mixture, H_2O_2 is needed as the oxidizing agent, where the semiconductor surface is first oxidized before this layer is etched by the SA. The etching mixture were prepared by liquefy 10 g of succinic acid granulates with 50 ml of DI water. Then, the mixture is diluted to pH 6 by Ammonium Hydroxide (NH_4OH), the same pH value previously used for Adipic Acid etchant [14]. From this solution, different set of solution were prepared by adding different H_2O_2 composition.

At this stage, the etching time was made constant for 5 minutes for all InGaAs samples. Since the etch rate of InAlAs is expected to be lower than 10 Å/min [12], the samples were left for 5 hours in the acid solution. The depth of etching was measured at five random locations using a Taylor Hobson's Talystep profiler (resolution = 2 nm) [15] after the resist layer is stripped-off. Thorough out this work, the etch rate is calculated by the average value of etch depth over the etching time in each solutions. The resulted etch rate for both InGaAs and InAlAs samples are illustrated in Fig. 4.

In the figure, the etch rate of InGaAs is showing decremting trend in increasing H_2O_2 volume. This trend is in agreement with H. Fourre et al [12] studies where the rate of surface oxidation increases as the peroxide volume increases. Thicker oxide layer can hardly be removed, slowing down the second reaction to take place, shown by shallower etch depth as peroxide volume increases. The graph also shows a turning point between 6.0 ml to 8.0 ml, where the etch rate fall by more than 50 Å/min. When the volume is < 6.0 ml and > 8.0 ml, the InGaAs etch rate is not a strong function of H_2O_2 composition. The etch rate for InAlAs is constant at ~ 2 Å/min throughout the first experiment, which confirms the purpose of the Aluminum element in the compound as the chemical etch stop layer. From this relationship, the selectivity of etchant can be calculated as in equation (1). The selectivity shows a declining trend, and is proportional to the InGaAs etching rate.

$$\text{Selectivity} = \frac{\text{InGaAs etch rate}}{\text{InAlAs etch rate}} \quad (1)$$

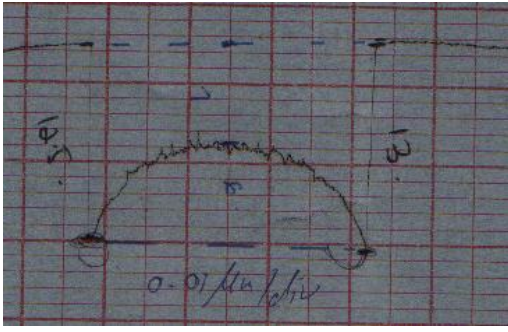


Fig. 5 Etch profile at InGaAs sample showing 0.01 μm/div

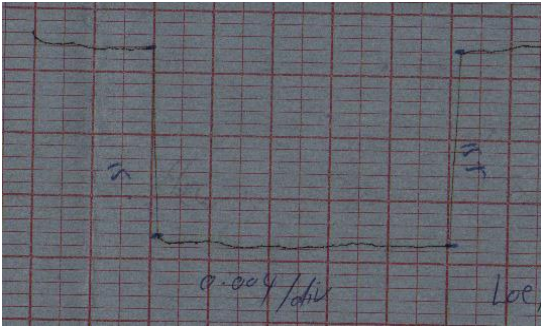


Fig. 6 Etch profile at InAlAs sample showing 0.004 μm/div

During the step profiling measurement, an important yet significant observation has been made particularly at the InGaAs samples. As shown in Fig. 5, there is a “hump” in the middle of the trench caused by the uncompleted etching reaction. This structure will be called “Dome Effect” hereafter. However, InAlAs shows clean and flat trenches etched profile (Fig. 6).

To examine the Dome Effect in the InGaAs layer, the percentage of dome height to etch depth is calculated. The graphical representation for the calculated percentage is shown in Fig. 7 and the calculation formula for Dome Effect is shown in equation (2). The persistence of doming effect can be viewed as the etchants etch away the crystalline materials at different rates depending upon which crystal face is exposed.

From the formula, the foreseen percentage can be viewed as the higher percentage, the higher the dome height relative to etch depth and thus the more prominent it is in the etching profile. Fig. 8 demonstrates the doming effect in InGaAs layers for different H₂O₂ composition. It can be seen that the dome height is around 40% to 50% over composition after five minutes etch time. Even though the percentage is stable, it raises a serious processing issue, as it will seriously damage the Schottky contact. Thus, experiments were carried out later not only to decide the best etchant composition, but also to address the elimination of “hump” structure in the InGaAs layers.

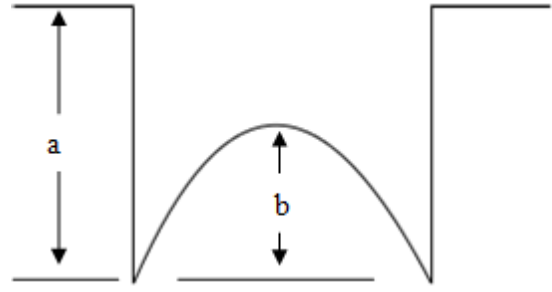


Fig. 7 Calculation for percentage of dome profile

$$\% \text{ of Dome Effect} = \frac{\text{Dome height, } b \text{ (Å)}}{\text{Etch depth, } a \text{ (Å)}} \quad (2)$$

The result from the first and the rest of the experiments, together with their finding are summarized in TABLE I. From the table, below are the important finding for etch rate and selectivity from each of the experiment:

1. H₂O₂: Moderate turning point of InGaAs etch rate at InGaAs samples at 6 ml and 8 ml. But changes is only ~ 60 Å/min
2. pH: The InGaAs etch rate decays exponentially while still preserving a low yet decreasing InAlAs etch rate along the pH variations. The result also shows that the pH values do have a strong relationship with the InAlAs etch rate.
3. DI: Significant turning point between high and low etch rate at InGaAs samples at 100 ml and 150 ml. A significant drop in selectivity at high buffering is also observed at 150 ml and 200 ml of H₂O volumes, where the selectivity drops from 137 to only about 30.

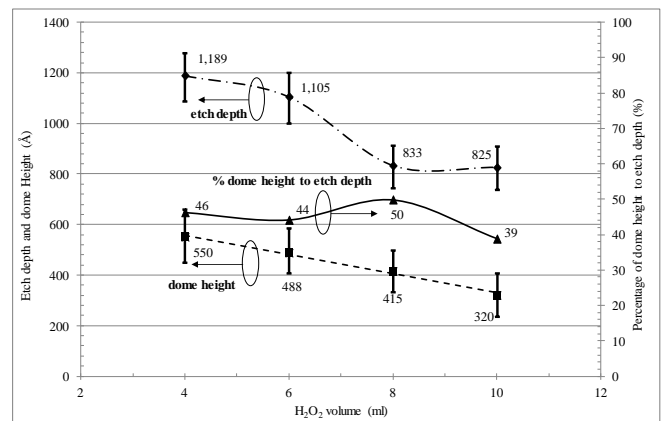


Fig. 8 Etching profile and percentage of Dome Effect of lattice matched InGaAs (DI volume = 50 ml, pH = 6.0 and etch time = 5 minutes)

TABLE I. SUMMARY OF EXPERIMENT

Test parameter	pH	H ₂ O ₂ (ml)	DI (ml)	Etch time	InGaAs trend	InAlAs trend	Selectivity	Dome Effect to etch depth (%)
H ₂ O ₂ composition	6	4 – 10 Interval = 2ml	50	5 min for InGaAs 5 hr for InAlAs	Turning point at 6-8 ml at 221 and 167 Å/min Constant before and after turning point	Constants at 2 Å/min	Turning point at 6-8 ml at 111 and 84 Constant before and after turning point	40 - 50
pH	5.0 – 6.5 Interval = 0.5	8	50	5 min for InGaAs 5 hr for InAlAs	Decreased exponentially from 865 to 77 Å/min	Decreased linearly from 9 to 1 Å/min	Peaks at pH 5.5 at 140	Increased linearly from 10 to 62
DI	6	5	50 – 200 Interval = 50 ml	5 min for InGaAs 5 hr for InAlAs	Turning point at 100 -150 ml at 260 and 68 Å/min. Constant before and after turning point	Constant at 2 Å/min	Turning point at 100 -150 ml at 137 and 35. Constant before and after turning point	Constant at 30 % until 100 ml and increase rapidly > 60 at high buffer

Fig. 9 shows the summary of the etchant composition to the % of Dome Effect. From the figure, one can conclude that to have a low percentage of Doming Effect, a solution with low pH value, low H₂O₂ composition and low DI water must be chosen while maintaining a high InGaAs-InAlAs etching selectivity. Failing to etch the InGaAs cap layer residue is a major cause for the failure in the Schottky contact behavior. Instead of acting as a Schottky barrier, the InGaAs residue will behave increasingly more like an Ohmic contact after heat treatment and thus deteriorate the device performances.

The final chemical composition is summarized in TABLE II. After considering all factor, these parameters are the most appropriate compositions for high selectivity and low Dome Effect percentage. As listed in the table, we used 5 ml of H₂O₂ for high InGaAs etch rate and high InGaAs-InAlAs selectivity. Additionally, a pH of 5.5 is chosen in order to have a low InAlAs etch rate and low Dome Effect percentage. Finally, low H₂O is chosen for high selectivity in addition to low Doming Effect percentage.

IV. CONCLUSIONS

A series of experiment procedures have been successfully presented in this paper to investigate the effect of each etching compound to the etching rate and indirectly the selectivity of InGaAs-InAlAs samples. At the end of experiment the optimal etching composition is chosen to be 5 ml of H₂O₂, pH of 5.5 and 50 ml of Deionized water. The etch rate for both materials and selectivity of the solution is approximately 2 Å/min for InAlAs, 240 Å/min for InGaAs and 140 respectively. Here, the percentage of Dome Effect is expected to be consistently 30%. The etching solution is suitable for reliable and highly reproducible pHEMT gate recess process, where the dome effect can be further eliminated by controlling the InGaAs etching time to the InAlAs etch stop layer.

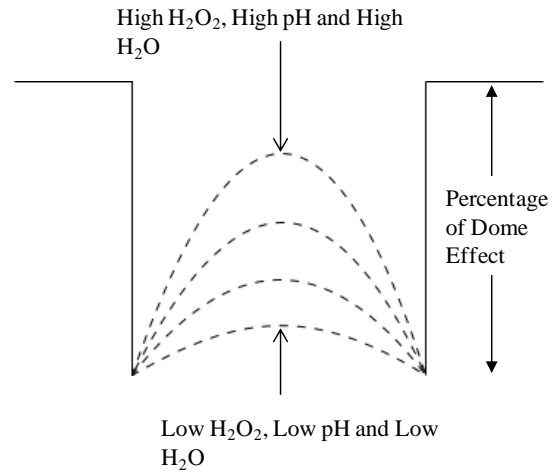


Fig. 9 Summary from chemical composition studies

TABLE II. FINAL ETCHING COMPOSITION

Parameter	Composition/value
Succinic acid granulates	10 g
H ₂ O ₂	5 ml
pH	5.5
H ₂ O	50 ml

REFERENCES

- [1] T. E. Whall and E. H. C. Parker, "SiGe heterostructures for FET applications," *Journal of Physics D: Applied Physics*, vol. 31, pp. 1397-1416, 1998.
- [2] E. Carey and S. Lidholm, *Millimeter-Wave Integrated Circuits*. Boston: Springer Science 2005.
- [3] M. J. W. Rodwell, et al., "III-V MOSFETs: Scaling laws, scaling limits, fabrication processes," in *Indium Phosphide & Related Materials (IPRM)*, 2010 International Conference on, 2010, pp. 1-6
- [4] Smith P Met al2001 *Advances in InP HEMT technology for high frequency applications*, IEEE Gallium Arsenide Integrated Circuit (GaAs IC) Symp. 2001 (Baltimore, MD), 23rd Annual Technical Digest.
- [5] G. Bauer and F. Schäffler, "Self-assembled Si and SiGe nanostructures: New growth concepts and structural analysis," *physica status solidi (a)*, vol. 203, pp. 3496-3505, 2006.
- [6] T. F. Kuech, et al., "Defect reduction in large lattice mismatch epitaxial growth through block copolymer full wafer patterning," in *Indium Phosphide & Related Materials*, 2009. IPRM '09. IEEE International Conference on, 2009, pp. 63-64.
- [7] G. C. Osbourn, "Strained layer superlattices from lattice mismatched materials," *Journal of Applied Physics*, vol. 53, pp. 1586-1589, 1982.
- [8] R. Chau, "Challenges and opportunities of emerging nanotechnology for VLSI nanoelectronics," in *Semiconductor Device Research Symposium*, 2007 International, 2007, pp. 1-1.
- [9] J.-H. Oh, et al., "Effects of the Gate Recess Structure on the DC Electrical Behavior of 0.1-um Metamorphic High-Electron-Mobility Transistors," *Journal of the Korean Physical Society*, vol. 45, p. 1004 to 1008, 2004
- [10] Y.-S. Lin, et al., "Effects of Selective and Nonselective Wet Gate Recess on InAlAs/InGaAs Metamorphic Field-Effect Transistors with Double Delta Doping in InGaAs Channels," *Journal of The Electrochemical Society*, vol. 158, pp. H305-H311, 2011.
- [11] T. P. E. Broekaert and C. G. Fonstad, "Novel, Organic Acid-Based Etchants for InGaAlAs/InP Heterostructure Devices with AlAs Etch-Stop Layers," *Journal of The Electrochemical Society*, vol. 139, pp. 2306-2309, 1992.
- [12] H. Fourre, et al., "Selective wet etching of lattice matched InGaAs/-InAlAs on InP and metamorphic InGaAs/InAlAs on GaAs using succinic acid/hydrogen peroxide solution," *Journal of Vacuum Science & Technology B: Microelectronics and Nanometer Structures*, vol. 14, pp. 3400-3402, 1996.
- [13] A. Bouloukou, et al., "Novel High-Breakdown InGaAs/InAlAs pHEMTs for Radio Astronomy Applications," presented at the 4th ESA Workshop on mm-Wave Technology and Applications, 2006
- [14] A. Bouloukou, et al., "Very low leakage InGaAs/InAlAs pHEMTs for broadband (300 MHz to 2 GHz) low-noise applications," *Materials Science in Semiconductor Processing*, vol. 11, pp. 390-393, 2008.
- [15] M. Jurzecka-Szymacha, et al., "Silicon nitride layers of various n-content: Technology, properties and structure," *Thin Solid Films*, vol. 520, pp. 1308-1312, 2011